

See discussions, stats, and author profiles for this publication at: <https://www.researchgate.net/publication/5952692>

# Encapsulation of Electron Donor–Acceptor Dyads in $\beta$ -Cyclodextrin Cavity: Unusual Planarization and Enhancement in Rate of Electron–Transfer Reaction

ARTICLE *in* THE JOURNAL OF PHYSICAL CHEMISTRY B · NOVEMBER 2007

Impact Factor: 3.3 · DOI: 10.1021/jp074643d · Source: PubMed

---

CITATIONS

15

---

READS

20

## 3 AUTHORS, INCLUDING:



**Mahesh Hariharan**

Indian Institute Of Science Education and Re...

45 PUBLICATIONS 843 CITATIONS

SEE PROFILE



**Prakash P Neelakandan**

University of Cambridge

16 PUBLICATIONS 462 CITATIONS

SEE PROFILE

# Encapsulation of Electron Donor–Acceptor Dyads in $\beta$ -Cyclodextrin Cavity: Unusual Planarization and Enhancement in Rate of Electron-Transfer Reaction

Mahesh Hariharan, Prakash P. Neelakandan, and Danaboyina Ramaiah\*

Photosciences and Photonics, Chemical Sciences and Technology Division, National Institute for Interdisciplinary Science and Technology, Council of Scientific and Industrial Research, Trivandrum 695 019, India

Received: June 15, 2007; In Final Form: August 6, 2007

Interaction of  $\beta$ -cyclodextrin ( $\beta$ -CD) with a few novel electron donor acceptor dyads **1a–c** and **2a–c**, having aryl and flexible methylene spacer groups, has been investigated through photophysical, chiroptical, electrochemical, NMR, and microscopic techniques. Dyads **1a** and **1c**, with *p*-tolyl and biphenyl spacer groups, respectively, exhibited significantly decreased fluorescence quantum yields and lifetimes in the presence of  $\beta$ -CD, while negligible changes were observed for dyad **1b** with an *o*-tolyl spacer. In contrast, spacer-length-dependent significant enhancement in fluorescence quantum yields and lifetimes was observed for dyads **2a–c**, with flexible polymethylene ( $n = 1, 3, 11$ ) spacer groups. Association constants of  $\beta$ -CD encapsulated complexes have been determined and the contrast behavior observed in these systems is explained through an electron transfer ( $k_{ET}$ ) mechanism based on calculated favorable change in free energy ( $\Delta G_{ET} = -1.27$  eV) and the redox species characterized through laser flash photolysis studies. Rates of  $k_{ET}$  have been estimated and are found to increase ca. 2-fold in the case of dyads **1a** and **1c** when encapsulated in  $\beta$ -CD, while significantly decreased  $k_{ET}$  values were observed for the dyads **2a–c** with flexible spacer (ca. 9-fold for **2c**). As characterized through cyclic voltammetry, 2D NMR [correlated (COSY) and nuclear Overhauser enhancement (NOESY) spectroscopy], and laser flash photolysis studies, the  $\beta$ -CD encapsulation of dyads with aliphatic spacer groups leads to the conformational unfolding of a sandwich type of structure, whereas dyads with rigid aryl spacer groups undergo unusual planarization as compared to the uncomplexed dyads, resulting in enhanced electron-transfer reaction between the donor and acceptor moieties.

## 1. Introduction

The study of interactions of cyclodextrins (CDs) with drugs and photoactive molecules has been an active area of research in recent years, as they mimic the biological environment.<sup>1</sup> Cyclodextrins are cyclic oligosaccharides consisting of 6–9 glucose units; they are called  $\alpha$ -,  $\beta$ -,  $\gamma$ -, and  $\delta$ -cyclodextrins, respectively.<sup>2</sup> CDs are water-soluble and have not only a rigid, well-defined torus shape with a relatively apolar interior<sup>3</sup> but also rotational symmetry with an asymmetric environment.<sup>1–3</sup> These cyclic systems are known to form inclusion complexes with a variety of compounds, ranging from low molecular weight nonpolar aliphatic molecules and polar amino acids to high molecular weight polymeric materials, depending on the size of the CD cavity and the cross-sectional area of the guest molecules.<sup>4</sup> Because of these unique properties, CDs have found wide applications in the pharmaceutical industry, catalysis, separation technology, and recently in the design of biomimetic systems, supramolecular architectures, and molecular machines.<sup>5</sup> Moreover, the hydrophobic and spatial control of CD inclusion processes has been extensively exploited not only for use as drug carriers,<sup>6</sup> in catalysis<sup>7</sup> and separation technology,<sup>8</sup> but also in controlling the reactivity and understanding the photochemical properties of a variety of functional molecules.<sup>9</sup> Of these systems, the electron donor–acceptor dyads<sup>10,11</sup> have attracted much attention, since inclusion of such systems in CDs not only alters the interactions between the donor and acceptor moieties

but also results in supramolecular architectures that are useful as molecular machines.<sup>12,13</sup>

The rate of intramolecular electron transfer ( $k_{ET}$ ) in a donor–acceptor conjugate is dependent on several parameters. These include free energy change, the distance between the donor and acceptor units, their nature and orientation, and the intervening medium.<sup>14</sup> Of these factors, the distance between the donor and acceptor, which also involves the nature of the spacer group, is the most important factor, because of the approximately exponential decrease of the rates with increasing distance.<sup>14,15</sup> Although the interactions of CDs with electron donor–acceptor dyads having flexible spacers have been reported,<sup>10,11,14–16</sup> the systems with sterically bulky and rigid aryl spacers have received less attention. Herein, we report the unusual effects of the spacer groups on  $\beta$ -cyclodextrin ( $\beta$ -CD) inclusion reactions of a few novel electron donor–acceptor conjugates **1a–c** and **2a–c** (Figure 1), which are biologically important and are efficient in cleaving DNA through the cosensitization mechanism.<sup>17</sup> Upon their inclusion in  $\beta$ -CD, we observed reduced  $k_{ET}$  for dyads **2a–c**, with flexible polymethylene spacer units, and negligible changes for **1b**, with a sterically bulky spacer group, but surprisingly enhanced  $k_{ET}$  for dyads **1a** and **1c**, with rigid aryl spacer groups. To the best of our knowledge, this is the first report that describes the unusual enhancement in electron-transfer reaction between the donor and acceptor moieties in dyads with rigid aryl spacer groups upon encapsulation in  $\beta$ -CD.

## 2. Experimental Section

**2.1. General Techniques.** The equipment and procedures for melting point determination and spectral recordings have been

\* To whom correspondence should be addressed: tel (+91) 471 2515362; fax (+91) 471 2490186 or 2491712; e-mail rama@csrrltd.ren.nic.in or d\_ramaiah@rediffmail.com.

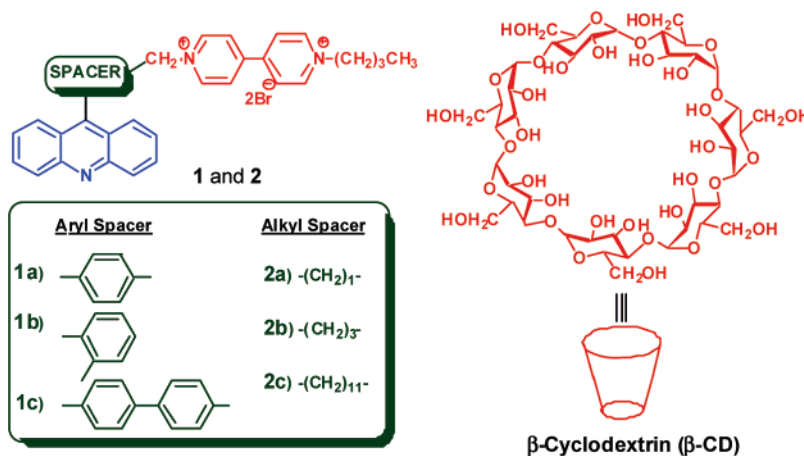


**Figure 1.** Structures of the viologen-linked acridine conjugates **1a–c** and **2a–c** and  $\beta$ -cyclodextrin ( $\beta$ -CD).

described.<sup>17</sup> An Elico pH meter was used for pH measurements.  $^1\text{H}$  and  $^{13}\text{C}$  NMR were measured on a 300 MHz Bruker advanced DPX spectrometer. Electronic absorption spectra were recorded on a Shimadzu UV–vis–near-IR spectrophotometer. Fluorescence spectra were recorded on a SPEX-Fluorolog F112X spectrofluorometer. The fluorescence quantum yields were determined by using optically matching solutions. 9-Aminoacridine in methanol ( $\Phi_f = 0.99$ ) was used as the standard.<sup>18</sup> Fluorescence lifetimes and anisotropy were measured on an IBH picosecond single photon counting system. The fluorescence and anisotropy decay profiles were deconvoluted by use of IBH Data Station software V2.1, fitted with a mono-, bi-, or triexponential decay with  $\chi^2$  values of the fit minimized to  $1 \pm 0.1$ . Laser flash photolysis experiments were carried out in an Applied Photophysics Model LKS-20 laser kinetic spectrometer by use of the third harmonic (355 nm, pulse width 20 ns) of a Quanta Ray GCR-12 series pulsed Nd:YAG laser. Circular dichroic spectra were recorded on a Jasco Corp. J-810 spectropolarimeter. Cyclic voltammetry was performed on a BAS CV50W cyclic voltammeter with sodium chloride as supporting electrolyte in aqueous medium. A standard three-electrode configuration was used with a glassy carbon working electrode, a platinum auxiliary electrode, and Ag/AgCl (3 M NaCl) reference electrode. The potentials were calibrated against the standard calomel electrode (SCE). Details of calculation of fluorescence quantum yields, rate of electron transfer, and association constants are given in the Supporting Information.

**2.2. Materials.** Diphenylamine,  $\beta$ -cyclodextrin ( $\beta$ -CD), and 1-adamantanecarboxylic acid (AD-COOH) were purchased from Aldrich and used without further purification. 4-Methyl-4'-biphenylcarboxylic acid, mp 168–169 °C (lit. mp 169 °C)<sup>19</sup> was prepared by modification of the reported procedures. 1-Butyl-4,4'-bipyridinium bromide was obtained in 95% yield by the reaction of 4,4'-bipyridine with 1-bromobutane in the molar ratio of 3:1 in dry acetonitrile. The viologen-linked acridine dyads **1a**, mp 268–269 °C (mixture mp);<sup>17</sup> **1b**, mp 224–225 °C (mixture mp);<sup>17</sup> **2a**, mp 260–261 °C (mixture mp);<sup>17</sup> **2b**, mp 253–254 °C (mixture mp);<sup>17</sup> and **2c**, mp 248–249 °C (mixture mp)<sup>17b</sup> were synthesized by modification of the earlier procedure.

**2.3. Synthesis of Dyad 1c.** A mixture of 4-methyl-4'-biphenylcarboxylic acid (1.42 mmol), diphenylamine (1.42 mmol), and anhydrous  $\text{ZnCl}_2$  (14 mmol) was heated at 230 °C for 24 h.  $\text{H}_2\text{SO}_4$  (20%, 20 mL) was added to the reaction mixture, which was refluxed for 4 h. It was then cooled and neutralized with 25% aqueous  $\text{NH}_3$  solution, and the solid product thus obtained was chromatographed over silica gel.

Elution of the column with a mixture (1:1) of ethyl acetate and hexane gave 9-(biphenyl-4-methyl)acridine in 10% yield after recrystallization from a mixture (1:9) of ethyl acetate and hexane, mp 267–269 °C:  $^1\text{H}$  NMR ( $\text{CDCl}_3$ , 300 MHz)  $\delta$  2.42 (3H, s), 7.31–8.17 (16H, m);  $^{13}\text{C}$  NMR ( $\text{CDCl}_3$ , 75 MHz)  $\delta$  21.1, 126.4, 127.4, 128.9, 129.8, 130.5, 131.1, 134.9, 135.9, 136.7, 138.2, 140.4, 143.3, 143.8. HRMS (ESI) calcd for  $\text{C}_{26}\text{H}_{19}\text{N}$ , 345.4358; found, 345.4367.

A mixture of 9-(biphenyl-4-methyl)acridine (0.1 mmol), *N*-bromosuccinimide (0.1 mmol), and 2,2'-azobisisobutyronitrile (AIBN) in 10 mL of dry  $\text{CCl}_4$  was refluxed for 12 h. After the reaction, the solution was filtered and allowed to crystallize. Product obtained was again recrystallized from  $\text{CCl}_4$  to give 54% 9-(4-bromomethylbiphenyl)acridine, mp 285–286 °C:  $^1\text{H}$  NMR ( $\text{CDCl}_3$ , 300 MHz)  $\delta$  4.56 (2H, s), 7.52–8.05 (16H, m);  $^{13}\text{C}$  NMR ( $\text{CDCl}_3$ , 75 MHz)  $\delta$  33.7, 126.7, 127.4, 128.5, 129.9, 130.5, 131.1, 134.9, 135.9, 138.2, 139.9, 142.1, 144.2, 145.8. HRMS (ESI) calcd for  $\text{C}_{26}\text{H}_{18}\text{BrN}$ , 424.3319; found, 424.3337.

To a solution of 9-(4-bromomethylbiphenyl)acridine (0.1 mmol) in dry acetonitrile (50 mL) was added 1-butyl-4,4'-bipyridinium bromide (0.1 mmol), and the mixture was stirred at room temperature for 12 h. Precipitated product was filtered and dried to give **1c**, which was recrystallized from a mixture (7:3) of methanol and ethyl acetate to give a 35% yield of the dyad **1c**, mp 291–293 °C:  $^1\text{H}$  NMR ( $\text{DMSO}-d_6$ , 300 MHz)  $\delta$  0.95 (3H, t,  $J = 7.4$  Hz), 1.35–1.38 (2H, m), 1.99–2.02 (2H, m), 4.79 (2H, t,  $J = 7.1$  Hz), 6.30 (2H, s), 7.37–8.27 (16H, m), 8.93–9.85 (8H, m);  $^{13}\text{C}$  NMR ( $\text{DMSO}-d_6$ , 75 MHz)  $\delta$  13.4, 18.8, 32.7, 60.6, 62.8, 109.1, 124.2, 126.2, 126.4, 126.8, 127.3, 128.3, 129.1, 129.3, 130.5, 131.1, 134.5, 136.2, 145.8, 146.0, 147.9, 148.6, 149.2. HRMS (ESI) calcd for  $\text{C}_{40}\text{H}_{35}\text{BrN}_3$ , 637.6301; found, 637.6315. Anal. Calcd for  $\text{C}_{40}\text{H}_{35}\text{Br}_2\text{N}_3$ : C, 66.96; H, 4.92; N, 5.86. Found: C, 66.74; H, 5.01; N, 5.96.

**2.4. Spectrophotometric and Spectrofluorometric Titrations.** The linearity of absorbance versus concentration was determined in the concentration range of ( $10^{-4}$ – $10^{-6}$  M) for all derivatives. Sample concentrations were taken between  $0.1 \times 10^{-5}$  and  $10 \times 10^{-5}$  M, where Beer's law was obeyed, and no aggregation of the solute in the aqueous solutions was found. The linearity of fluorescence emission vs concentration was also checked in the same concentration range used. The absorbance at the excitation wavelength was maintained lower than 0.15. Titrations of  $\beta$ -cyclodextrin with the donor–acceptor dyads were carried out in aqueous medium. Aliquots (3 mL) of these dyads were taken in a quartz cuvette, with concentrations ranging  $0.1 \times 10^{-5}$  to  $10 \times 10^{-5}$  M. Subsequently, a 0.090 M stock solution of  $\beta$ -cyclodextrin was added in 20–200  $\mu\text{L}$  volume to 3 mL of

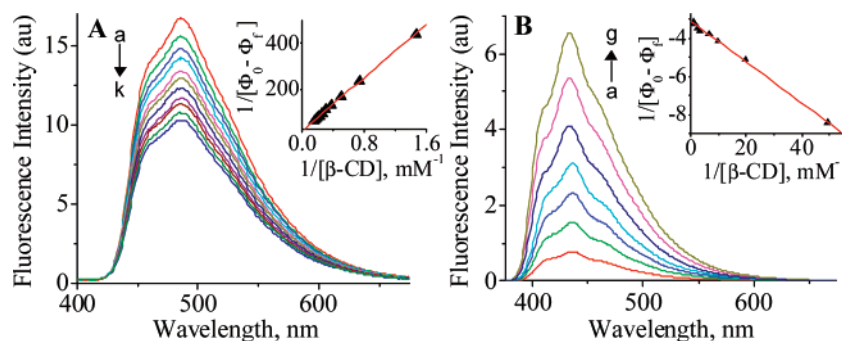


**Figure 2.** Change in fluorescence spectra of (A) **1a** ( $4.1 \times 10^{-5}$  M) and (B) **2c** ( $4.1 \times 10^{-5}$  M); as a function of  $\beta$ -CD concentration in aqueous medium. (A)  $[\beta\text{-CD}] =$  (a) 0, (b) 0.68, (d) 2.01, (g) 3.94, and (k) 6.40 mM; (B)  $[\beta\text{-CD}] =$  (a) 0, (b) 0.02, (e) 0.07 and (g) 0.09 mM. (Insets) Corresponding Benesi–Hildebrand plots. Excitation wavelength was 360 nm.

**TABLE 1: Fluorescence Quantum Yields ( $\Phi$ ) and Lifetimes ( $\tau$ ) and Association Constants ( $K_{\text{assn}}$ ) of Complexes Formed between  $\beta$ -Cyclodextrin and Dyads **1a–c** and **2a–c**<sup>a</sup>**

dyad	$\Phi \times 10^2$	$\Phi_{\beta\text{-CD}} \times 10^2$	$\tau$ , ns	$\tau_{\beta\text{-CD}}$ , ns	$K_{\text{assn}}$ , <sup>b</sup> M <sup>−1</sup>
<b>1a</b>	$0.60 \pm 0.04$	$0.34 \pm 0.02$	5.4 (100%)	5.4 (69%), 0.9 (31%)	$239 \pm 5^c$
<b>1b</b>	$0.08 \pm 0.05$	nc <sup>d</sup>	10.6 (87%), 0.40 (13%)	nc	nb <sup>e</sup>
<b>1c</b>	$0.71 \pm 0.03$	$0.35 \pm 0.03$	5.7 (100%)	5.7 (40%), 1.4 (60%)	$325 \pm 6$
<b>2a</b>	$0.70 \pm 0.05$	$1.06 \pm 0.04$	14.6 (100%)	15.0 (100%)	$36 \pm 2$
<b>2b</b>	$0.20 \pm 0.03$	$1.62 \pm 0.05$	13.6 (81%), 2.80 (19%)	15.5 (82%), 5.80 (18%)	$219 \pm 6$
<b>2c</b>	$10 \pm 0.10$	$91 \pm 0.06$	14.7 (82%), 1.70 (18%)	15.0 (82%), 8.30 (18%)	$29600 \pm 100$

<sup>a</sup> Average of more than three experiments. <sup>b</sup>  $K_{\text{assn}}$  was calculated using Benesi–Hildebrand equation. <sup>c</sup> <sup>1</sup>H NMR titrations gave  $K_{\text{assn}} = 337 \pm 9$  and  $224 \pm 12$  M<sup>−1</sup> for **1a** and **2b**. <sup>d</sup> Negligible changes were observed. <sup>e</sup> Negligible binding was observed.

these dyads. A series of <sup>1</sup>H NMR spectra were recorded upon addition of 50  $\mu$ L of 8.7 mM stock solution of  $\beta$ -cyclodextrin to 0.75 mL of dyads in D<sub>2</sub>O.

### 3. Results

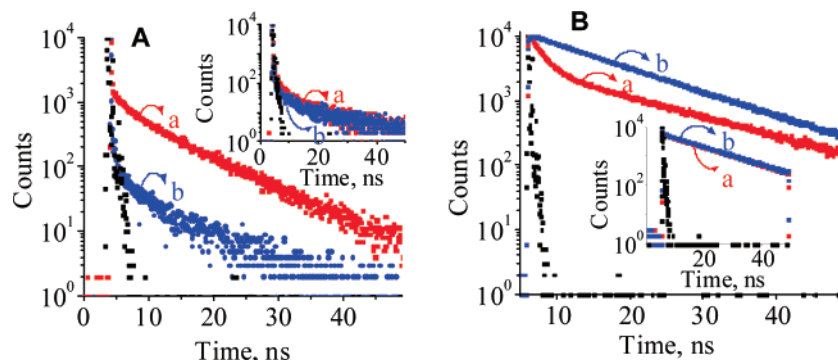
**3.1. Interactions of Donor–Acceptor Dyads with  $\beta$ -Cyclodextrin.** Synthesis of the viologen-linked acridine conjugates **1a,b** and **2a–c** has been achieved through modification of the earlier procedure,<sup>17</sup> while **1c** was synthesized in moderate yields by the quaternization of the corresponding acridine derivative with monobutylbipyridinium bromide. All these compounds were purified through recrystallization and characterized on the basis of spectral data and analytical evidence. These conjugates exhibited high solubility in aqueous medium and obeyed Beer’s law under our experimental conditions. We observed no evidence for ground-state charge-transfer interaction between the acridine chromophore and viologen moiety present in these compounds in aqueous and buffer media.

Figure 2A shows the change in fluorescence spectra of dyad **1a** as a function of increasing concentration of  $\beta$ -CD. Upon increasing  $\beta$ -CD concentration, we observed a regular decrease in the fluorescence intensity corresponding to the acridine chromophore. Similar observations were made with dyad **1c** containing the biphenyl spacer group (Figure S1, Supporting Information). However, with the addition of  $\beta$ -CD, negligible changes were observed in the absorption spectra of dyads **1a** and **1c** and also in the absorption and fluorescence spectra of dyad **1b** with an *o*-tolyl spacer group (Figures S2 and S3, Supporting Information). On the other hand, donor–acceptor dyads **2a–c**, with flexible polymethylene spacer groups (methylene units of  $n = 1, 3$  and  $11$ ; Figure 2B and Figures S4 and S5, Supporting Information), exhibited spacer-length-dependent increases in fluorescence intensity with increasing concentration

of  $\beta$ -CD. For example, in the case of viologen-linked acridine conjugate **2c**, we observed ca. 9-fold enhancement in the fluorescence intensity with the addition of 0.09 mM  $\beta$ -CD.

Benesi–Hildebrand analysis of the fluorescence changes (insets of Figures 2, S1, S4, and S5) gave a 1:1 stoichiometry for the complexes formed between  $\beta$ -CD and dyads **1a, 1c**, and **2a–c**. The **1a**/ $\beta$ -CD complex showed an association constant ( $K_{\text{assn}}$ ) of 239 M<sup>−1</sup> with the corresponding change in free energy value of  $-13.7$  kJ mol<sup>−1</sup>. The association constants and fluorescence lifetimes of these dyads in the presence and absence of  $\beta$ -CD are summarized in Table 1. In the case of dyad **1c**, with a biphenyl spacer group, we observed an association constant of 325 M<sup>−1</sup>, whereas dyad **2c**, with a polymethylene flexible spacer length of  $n = 11$ , exhibited nearly ca. 124-fold higher association constant ( $K_{\text{assn}} = 29600$  M<sup>−1</sup>), as compared to **1a**. In order to evaluate the thermodynamic parameters, we have determined the association constants of a few representative systems at different temperatures. We observed  $\Delta H^0 = -4.1$  kJ mol<sup>−1</sup> and  $\Delta S^0 = 71.8$  J K<sup>−1</sup> mol<sup>−1</sup> for dyad **2c** ( $n = 11$ ), while **2b** ( $n = 3$ ) exhibited values of  $\Delta H^0 = -10.6$  kJ mol<sup>−1</sup> and  $\Delta S^0 = 8.6$  J K<sup>−1</sup> mol<sup>−1</sup>, indicating thereby that entropic gain for association of dyad **2b** with  $\beta$ -CD is much lower as compared with dyad **2c**. The observed 8-fold higher value of change in entropy upon complexation of  $\beta$ -CD with dyad **2c**, as compared with dyad **2b**, could be due to desolvation of the flexible spacer ( $n = 11$ ) and/or greater conformational mobility of the donor and acceptor units of the dyad. Further, the favorable change in enthalpy of complexation observed in both these dyads confirms the involvement of effective van der Waals interactions between the spacer groups and the hydrophobic cavity of  $\beta$ -CD. The higher value of change in enthalpy (2.5-fold) observed for the complex between  $\beta$ -CD and **2b**, when





**Figure 3.** Fluorescence decay profiles of (A) **1a** (1.23  $\mu$ M), (A, inset) **1b** (1.23  $\mu$ M), (B) **2c** (1.57  $\mu$ M), and (B, inset) **2a** (1.91  $\mu$ M) in aqueous medium, (a) in the absence and (b) in the presence of  $\beta$ -CD. Excitation and emission wavelengths were 360 and 485 nm, respectively.

compared with dyad **2c**, could be attributed to the stable and relatively rigid complex formed in the former case.

To have a better understanding of the fluorescence changes observed in the presence of  $\beta$ -CD, we have analyzed the interaction of  $\beta$ -CD with dyads **1a–c** and **2a–c** by picosecond time-resolved fluorescence techniques. As shown in Figure 3A, dyad **1a** exhibited a monoexponential decay with a lifetime of 5.4 ns in the aqueous medium, whereas a biexponential decay with lifetimes of 0.9 ns (31%) and 5.4 ns (69%) (Table 1) was observed in the presence of  $\beta$ -CD. Similar observations were made with dyad **1c** containing the biphenyl spacer group. Dyad **1c**, which showed a monoexponential decay with a lifetime of 5.7 ns, exhibited a biexponential decay with lifetimes of 1.4 ns (60%) and 5.7 ns (40%) in the presence of  $\beta$ -CD. On the other hand, negligible changes were observed for dyad **1b**. In contrast, dyads **2a–c**, with flexible polymethylene spacer groups, showed enhancement in lifetimes in the presence of  $\beta$ -CD (Figure 3B). For example, dyad **2a**, which showed a monoexponential decay with a lifetime of 14.6 ns, exhibited a marginal enhancement in lifetime (15 ns) when complexed with  $\beta$ -CD (Figure 3B, inset). Dyad **2c**, with a long flexible spacer length of  $n = 11$ , on the other hand, showed biexponential decay with lifetimes of 14.7 and 1.7 ns (Figure 3B), while in the presence of  $\beta$ -CD, it exhibited significantly enhanced lifetimes of 15.0 and 8.3 ns. As indicated above, of the two lifetimes of dyads **2b** and **2c**, only the short-lived component exhibited significantly increased lifetimes in the presence of  $\beta$ -CD as compared to the long-lived major component (Table 1).

Intramolecular electron-transfer rates ( $k_{ET}$ ) of dyads in the presence and absence of  $\beta$ -CD have been estimated from the fluorescence quantum yields and lifetimes.<sup>17</sup> Unusually,  $k_{ET}$  for dyad **1a** with a *p*-tolyl spacer group increased from  $1.16 \times 10^{10} \text{ s}^{-1}$  in the aqueous medium to  $2.03 \times 10^{10} \text{ s}^{-1}$  in the presence of  $\beta$ -CD. Similarly, ca. 2-fold enhancement in  $k_{ET}$  was observed for dyad **1c**, containing a biphenyl spacer group, upon encapsulation in  $\beta$ -CD. In contrast, dyads **2a–c**, with flexible polymethylene spacer groups, showed significantly reduced  $k_{ET}$  values upon encapsulation in  $\beta$ -CD. For example, dyad **2c** ( $n = 11$ ), which exhibited  $k_{ET} = 0.6 \times 10^9 \text{ s}^{-1}$  in aqueous medium, showed significantly reduced  $k_{ET}$  values, by 1 order of magnitude, upon encapsulation in  $\beta$ -CD ( $k_{ET} = 0.4 \times 10^8 \text{ s}^{-1}$ ). To understand the contrasting behavior of dyads with flexible and rigid aryl spacer groups in the presence of  $\beta$ -CD, we have investigated their interactions in an alternative microenvironment medium such as micelles. Interestingly, irrespective of the nature of the spacer group, dyads **1a–c** and **2a–c** showed enhancement in the fluorescence quantum yields and lifetimes in the presence of SDS micelles (Figures S6, Supporting Information).

**3.2. Characterization of  $\beta$ -Cyclodextrin Inclusion Complexes.** Evidence for complexes formed between  $\beta$ -CD and

electron donor–acceptor dyads **1a**, **1c**, and **2a–c** was obtained by time-resolved fluorescence anisotropy, circular dichroism (CD), competitive ligand displacement,  $^1\text{H}$  NMR, and cyclic voltammetry (CV) techniques. Fluorescence anisotropy gives a physical insight to the extent of restriction imposed by the microenvironment on the dynamics of the molecule; thus it can be exploited for confirming the formation of stable inclusion complexes with  $\beta$ -CD.<sup>20</sup> Time-resolved anisotropy studies of dyad **1a**, with a *p*-tolyl spacer group, in the presence of  $\beta$ -CD showed monoexponential decay with a rotational correlation time of 0.37 ns and  $r_0$  value of 0.03–0.05 (Figure S7, Supporting Information). The calculated value for a hydrodynamic radius of 1:1 complex formed between **1a** and  $\beta$ -CD, by use of the rotational correlation time, was found to be  $7.2 \pm 0.5 \text{ \AA}$ , which corresponds to a diameter of  $14.4 \pm 0.5 \text{ \AA}$ , indicating the formation of a tight complex between  $\beta$ -CD and dyad **1a**, having a diameter of 14.9  $\text{\AA}$ . This is supported by evidence from circular dichroic studies. Dyad **1a**, which is inherently CD-inactive in the aqueous medium, showed an induced CD (ICD) signal corresponding to the acridine chromophore when  $\beta$ -CD (6.4 mM) was added (Figure S8, Supporting Information).<sup>21</sup> As expected, dyad **1b**, with an *o*-tolyl spacer group, showed no anisotropic behavior or ICD signal in the presence of  $\beta$ -CD, confirming its inability to undergo encapsulation inside the chiral  $\beta$ -CD cavity.

Ligand displacement technique is a widely used methodology to confirm host–guest complexation, particularly for characterizing the encapsulation of a guest molecule inside the host cavity.<sup>22</sup> To understand the interactions of dyads **1a**, **1c** and **2a–c** with  $\beta$ -CD, we employed 1-adamantanecarboxylic acid (AD-COOH),<sup>23</sup> a known  $\beta$ -CD encapsulating agent with an association constant of  $K_{\text{assn}} = 1.14 \times 10^3 \text{ M}^{-1}$ . Figure 4 shows the competitive displacement of dyad **1a** from the **1a**/ $\beta$ -CD complex by AD-COOH. Addition of  $\beta$ -CD results in significant quenching of fluorescence intensity of dyad **1a**, followed by saturation at ca. 6.4 mM  $\beta$ -CD. When AD-COOH was gradually added to this **1a**/ $\beta$ -CD complex, we observed quantitative revival of the fluorescence intensity of the conjugate, confirming thereby the effective displacement of dyad **1a** by AD-COOH from the  $\beta$ -CD cavity.

Figure 5A shows  $^1\text{H}$  NMR spectra of **1a** with gradual addition of  $\beta$ -CD. In the presence of  $\beta$ -CD, dyad **1a** showed significant changes in chemical shift ( $\Delta\delta = 0.3$ ), of the proton corresponding to the spacer phenyl group. Analysis of the chemical shift changes through a Benesi–Hildebrand plot (Figure 5B) gave an association constant of  $337 \pm 12 \text{ M}^{-1}$  for **1a**, which is marginally higher than the value obtained by fluorescence titrations. In contrast, the NMR spectrum of dyad **1b**, with the *o*-tolyl spacer group, showed negligible changes in the presence of  $\beta$ -CD. The cyclic voltammogram of **1a**, with a rigid extended

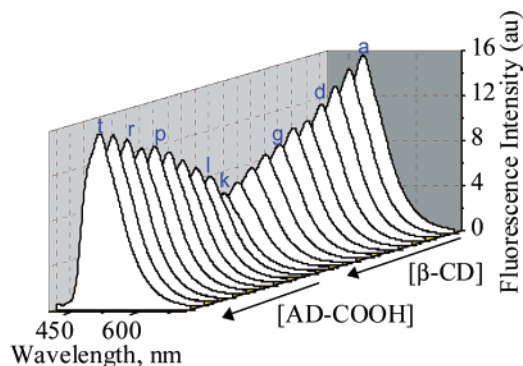


**Figure 4.** Fluorescence spectra of **1a** ( $4.1 \times 10^{-5}$  M) with increasing concentration of  $\beta$ -CD in aqueous medium— $[\beta\text{-CD}] =$  (a) 0, (d) 2.01, (g) 3.94, and (k) 6.40 mM—followed by gradual addition of AD-COOH— $[\text{AD-COOH}] =$  (l) 0.12, (p) 0.61, (r) 0.85, and (t) 1.21 mM. Excitation wavelength was 360 nm.

conformation, exhibited two reversible one-electron reduction processes centered at  $-0.44$  and  $-0.73$  V, characteristic of the viologen moiety (Figure S9, Supporting Information). With increasing addition of  $\beta$ -CD, we observed an increase in the reduction potentials by 66 and 10 mV, along with significant decreases in current intensity of  $35.7 \mu\text{A}$  (71%) and  $15.7 \mu\text{A}$  (61%), respectively.<sup>24</sup> In contrast, dyad **2b** showed only one reversible one-electron reduction process centered at  $-0.54$  V.<sup>25</sup> This behavior could be attributed to the existence of a folded sandwich-type conformation for dyad **2b**, in which both the donor acridine and acceptor viologen moieties are in close proximity.<sup>24,25</sup> In the presence of  $\beta$ -CD, a decrease in the reduction potentials by 38 mV (Figure S9 inset), along with a significant decrease in current intensity of  $6 \mu\text{A}$  (39%) was observed for **2b**, indicating thereby the formation of stable  $\beta$ -CD encapsulated complexes.

**3.3. Evidence for Electron-Transfer Reaction and Relative Planarization of the Dyad upon  $\beta$ -CD Encapsulation.** The feasibility of electron transfer between the acridine chromophore and viologen moiety was determined by fluorescence titration experiments as well as by characterizing the transient intermediates through laser flash photolysis studies.<sup>17</sup> Direct laser excitation of the viologen-linked acridine conjugates **1a–c** and **2a–c** (355 nm, pulse width 20 ns) in aqueous medium did not show any transients. However, in the presence of an external donor such as guanosine, characteristic transient absorptions due to the redox species were observed. This observation can be attributed to the existence of a fast charge recombination reaction in these covalently linked systems, and the presence of a sacrificial electron donor was found to stabilize the charge-separated species. For example, the transient absorption spectrum obtained immediately after laser excitation of dyad **1a** in the presence of guanosine exhibited three absorption maxima at 395, 525, and 610 nm and consisted of two transient species (Figure S10, Supporting Information). The first transient, with two maxima at 395 and 610 nm, exhibited a first-order growth rate constant of  $4.8 \times 10^4 \text{ s}^{-1}$ , while the second transient, with absorption maximum at 525 nm, exhibited a first-order decay constant of  $2.1 \times 10^4 \text{ s}^{-1}$ . As per the experimental and literature evidence,<sup>17,26</sup> the first species could be assigned to the reduced viologen radical cation, while the latter species is due to formation of the guanosine radical cation. Similar observations have been made in the case of dyads **1b,c** and **2a–c**.

Figure 6 shows the transient absorption spectrum obtained upon laser excitation of  $\beta$ -CD-encapsulated dyad **1a** in the presence of guanosine. As observed in the absence of  $\beta$ -CD, the transient absorption spectrum showed three absorption

maxima at 395, 525, and 610 nm, indicating the formation of radical cations of reduced viologen as well as guanosine. However, the rate of formation of the reduced viologen radical cation (absorption maxima at 395 and 610 nm) was found to be ca. 2-fold higher ( $7.7 \times 10^4 \text{ s}^{-1}$ ) than that observed in the absence of  $\beta$ -CD. The guanosine radical cation (absorption maximum 525 nm), on the other hand, showed nearly the same decay rate in the presence and absence of  $\beta$ -CD ( $2.7 \times 10^4 \text{ s}^{-1}$ ).

Further evidence for formation of the encapsulated complex as well as relative planarization of dyad **1a** inside the  $\beta$ -CD cavity was obtained through 2D NMR [correlated (COSY) and nuclear Overhauser enhancement (NOESY) spectroscopy] techniques.<sup>27</sup> Figure 7 shows the 2D NOESY spectra of viologen-linked acridine dyad **1a** in the absence and presence of  $\beta$ -CD in  $\text{D}_2\text{O}$  at 25 °C. In the absence of  $\beta$ -CD, no NOE cross-coupling peaks were observed in the aromatic region (Figure 7B). In contrast, in the presence of  $\beta$ -CD, several NOE peaks (blue peaks are NOE-positive) corresponding to the aromatic protons of dyad **1a** were observed (Figure 7C). In particular, strong NOE cross-coupling was observed between  $\text{H}_g$  protons of the acridine chromophore ( $\delta = 7.5$ ) and  $\text{H}_f$  protons of the aryl spacer group ( $\delta = 7.1$ ) and between  $\text{H}_e$  protons of the aryl spacer ( $\delta = 7.55$ ) and  $\text{H}_d$  protons of one of the bipyridyl units ( $\delta = 7.15$ ). Furthermore, upon encapsulation of dyad **1a** in  $\beta$ -CD, we observed strong NOE cross-coupling peaks between  $\text{H}_b$  ( $\delta = 9.2$ ) and  $\text{H}_c$  ( $\delta = 8.7$ ) protons of both pyridyl units of the viologen moiety. The observation of NOE cross-coupling interactions in the presence of  $\beta$ -CD plausibly reflects the relative planarization of the dyad inside the  $\beta$ -CD cavity, as compared to the free dyad, resulting in strong through-space interactions between protons of the acridine chromophore, the aryl spacer group, and the viologen moiety. Moreover, the complexed state can undergo hydrogen-bonding interactions between hydrogen atoms of the acridine moiety and hydroxyl groups of  $\beta$ -CD, resulting in a more stable complex. Such interactions between the dyad and  $\beta$ -CD could result in a relatively planarized conformation when compared to the dyad in the aqueous medium.

## 4. Discussion

For compounds in which a donor and an acceptor are separated by flexible or rigid spacer groups, the dependence of electron-transfer reactions on distance is well documented.<sup>14,28–31</sup> In such systems, both through-bond and through-space interactions play a key role in determining the photophysical properties. In the case of viologen-linked acridine dyads **1a–c** and **2a–c**, the observation of low fluorescence quantum yields is explained by an electron-transfer mechanism based on calculated favorable change in free energy of  $\Delta G = -1.27$  eV and the redox species characterized through laser flash photolysis studies. The observed decrease in the value of  $k_{\text{ET}} = 1.16 \times 10^{10} \text{ s}^{-1}$  for dyad **1a**, having a *p*-tolyl spacer, compared to **1b**, with an *o*-tolyl spacer ( $k_{\text{ET}} = 8.8 \times 10^{10} \text{ s}^{-1}$ ), indicates the importance of conformation for an effective through-space interaction. In the case of dyads with flexible spacer units, we observed a value of  $k_{\text{ET}} = 1.06 \times 10^{10} \text{ s}^{-1}$  for **2a** ( $n = 1$ ), while **2c**, with a longer spacer unit ( $n = 11$ ), exhibited ca. 9-fold lower value ( $k_{\text{ET}} = 1.12 \times 10^9 \text{ s}^{-1}$ ), which indicates a decrease in intramolecular electron-transfer rate with increasing spacer length.

Upon  $\beta$ -CD encapsulation, dyads **1a** and **1c**, showed decreased fluorescence yields and lifetimes (fluorescence OFF, Figure 8), whereas dyads **2a–c** showed spacer-length-dependent enhancement in the fluorescence quantum yields and lifetimes

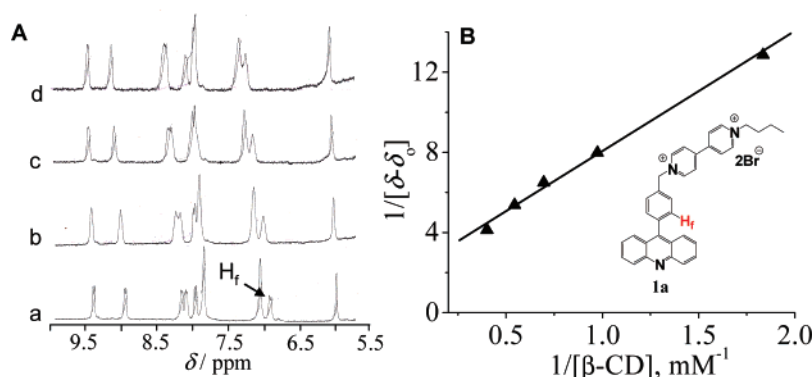


**Figure 5.** (A)  $^1\text{H}$  NMR spectra of **1a** (37.2 mM) with increasing addition of  $\beta$ -CD in  $\text{D}_2\text{O}$ :  $[\beta\text{-CD}] =$  (a) 0, (b) 1.03, (c) 1.45, and (d) 2.49 mM. (B) Benesi–Hildebrand plot of change in chemical shift of the phenyl proton  $\text{H}_f$  of **1a**.

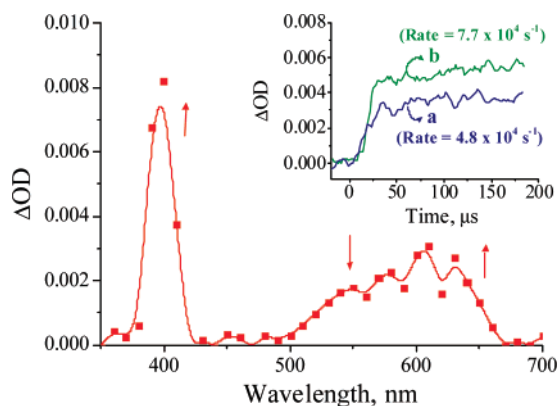


**Figure 6.** Transient absorption spectrum of **1a** ( $5.6 \times 10^{-5}$  M) in the presence of guanosine (1 mM) and  $\beta$ -cyclodextrin (6.4 mM) in aqueous medium recorded at 150  $\mu\text{s}$  after 355 nm laser excitation. (Inset) Growth of the reduced viologen radical cation at 395 nm (a) in the absence and (b) in the presence of  $\beta$ -CD.

(fluorescence ON, Figure 8). The observation of significantly decreased fluorescence yields in the case of **1a** and **1c** is intriguing, and on the basis of experimental evidence, it is attributed to the increased rate of electron-transfer reaction due to encapsulation in the  $\beta$ -CD cavity. Consistent with this assignment, no significant changes were observed with *o*-tolyl-containing **1b**, which exhibited negligible interactions with  $\beta$ -CD. This plausibly reflects that dyads **1a** and **1c**, upon  $\beta$ -CD encapsulation, undergo relative planarization inside the cavity, thereby resulting in the enhanced rate of electron-transfer reaction between donor and acceptor moieties. To support this view, in the presence of  $\beta$ -CD, significantly increased reduction potentials and ca. 2-fold increase in the rate of formation of the reduced viologen radical cation were observed, when compared to the absence of  $\beta$ -CD. The calculated excited-state deactivation rate constants of dyad **1a** in the absence ( $k_{\text{SI}} = 1.17 \times 10^{10} \text{ s}^{-1}$ ) and presence ( $k_{\text{SI}} = 2.05 \times 10^{10} \text{ s}^{-1}$ ) of  $\beta$ -CD further confirm that the electron-transfer reaction is the predominant deactivation pathway of the singlet excited states in these cases. In contrast, encapsulation of dyads **2a–c**, with flexible spacer groups, hinders the interaction between donor and acceptor moieties, thereby resulting in decreased rates of electron transfer, which is in accordance with the observations made for such donor–acceptor systems.<sup>10,11</sup> Moreover, all these dyads **1a–c** and **2a–c** exhibited similar fluorescence enhancement and lifetimes in the presence of micelles such as sodium dodecyl sulfate, confirming that all these systems undergo microencapsulation in micelles, whereas dyads **1a** and **1c**, with rigid aryl spacer groups, undergo unusual relative planarization inside the  $\beta$ -CD cavity.

As is evident from the photophysical, electrochemical, and chiroptical results, the dyads form tight 1:1 complexes with  $\beta$ -CD through inclusion of aryl or polymethylene spacer groups in the hydrophobic  $\beta$ -CD cavity. This is based on the following experimental facts: (i) observation of the induced CD signal corresponding to the acridine chromophore upon  $\beta$ -CD encapsulation, (ii) good agreement of the calculated hydrodynamic diameter of  $14.4 \pm 0.4 \text{ \AA}$  from the anisotropy measurements with the theoretically calculated molecular length of 14.9  $\text{\AA}$ , (iii) competitive displacement of  $\beta$ -CD-encapsulated dyad **1a** by a known binding agent such as AD-COOH, (iv) observation of significant changes in chemical shift of the aryl/alkyl protons of the spacer groups, and (v) decrease in current intensity in the presence of  $\beta$ -CD.

The acridine chromophore of dyads **1a**, **1c**, and **2a–c** can in principle undergo interactions with  $\beta$ -CD along its long molecular axis (radius = 9.19  $\text{\AA}$ );<sup>32</sup> however, substitution at the ninth position prevents it from such interactions due to steric reasons (Figure 8). Therefore,  $\beta$ -CD binds to these dyads initially through the viologen unit, leading to a less stable transition state<sup>33</sup> and then finally the complexed state, where  $\beta$ -CD is located on the spacer group. Dyad **1a**, with a length of 5.84  $\text{\AA}$  and width of 4.30  $\text{\AA}$ , undergoes effective  $\beta$ -CD encapsulation, whereas **1b**, with an *o*-tolyl spacer, is incapable of interacting with  $\beta$ -CD due to the bulkiness of the substituent. Free energy changes observed during the  $\beta$ -CD complexation are found to be favorable for **1a** and **1c**, while in the case of **2a–c**, the free energy increases with increasing spacer length. This could be attributed to the increase in entropy due to the displacement of water molecules from the  $\beta$ -CD cavity by guest molecules. The observed spacer-length-dependent increase in association constants and changes in chemical shifts of the spacer group confirm the involvement of flexible methylene groups in the formation of inclusion complexes between **2a–c** and  $\beta$ -CD.

Observation of (i) ca. 2-fold enhancement in the rate of electron-transfer reaction, (ii) significantly increased reduction potential of the viologen moiety, and (iii) increased rate of formation of the reduced viologen radical cation (around 2-fold) in the case of dyads **1a** and **1c** in the presence of  $\beta$ -CD could be due to the change in dielectric constant of the medium and/or formation of a relatively planarized conformer upon  $\beta$ -CD encapsulation. In the absence of  $\beta$ -CD, the spacer is exposed to the aqueous medium, which has a high dielectric constant, whereas upon encapsulation in  $\beta$ -CD, the spacer is in the relatively nonpolar interior of  $\beta$ -CD. In principle, this can decrease the local dielectric constant of the medium at the donor and acceptor moieties in the presence of  $\beta$ -CD, leading to an enhanced rate of electron transfer. Though the effect of change



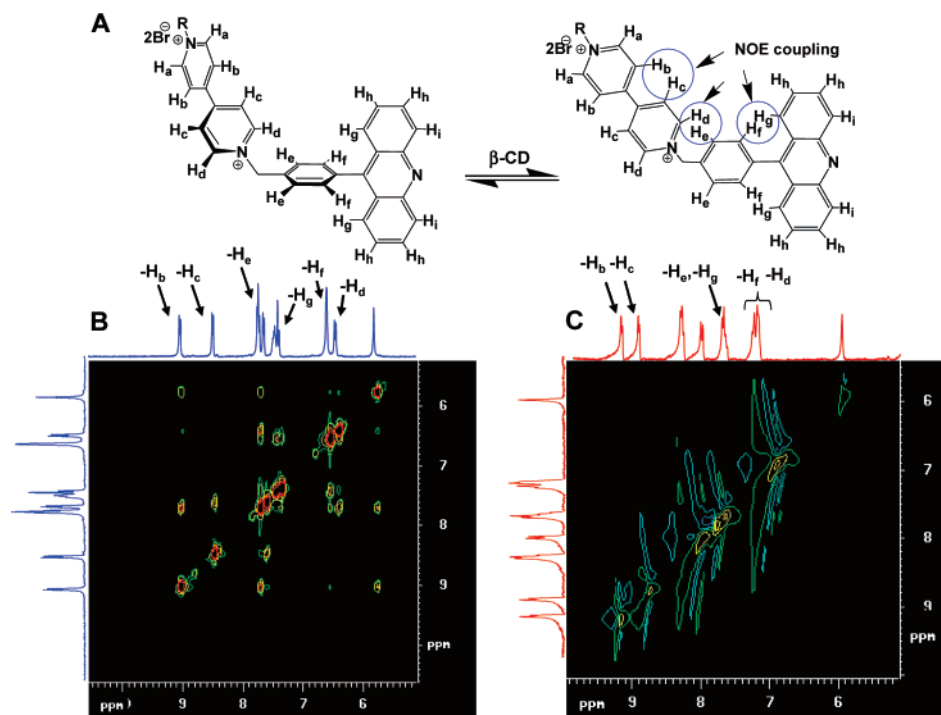


**Figure 7.** (A) Schematic illustration of planarization of the dyad **1a** in presence of  $\beta$ -CD with labeled aromatic protons. (B, C) Partial NOESY spectra of **1a** (37.2 mM), (B) in D<sub>2</sub>O and (C) in the presence of  $\beta$ -CD (5 mM).

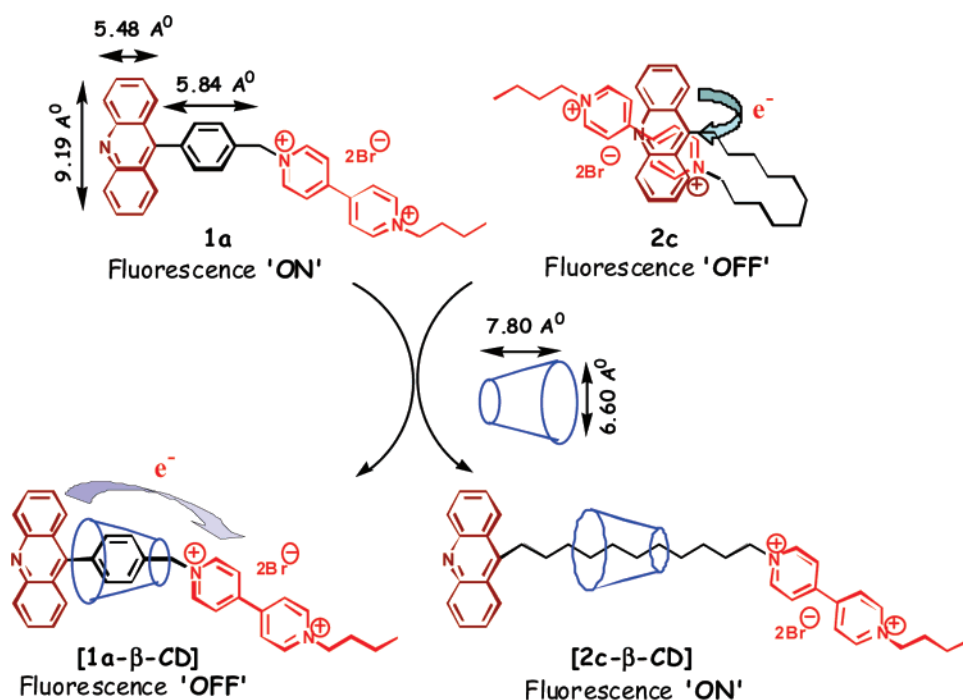


**Figure 8.** Schematic illustration of interactions between  $\beta$ -CD and the donor acceptor dyads **1a**, with rigid aryl spacer groups, and **2c**, with flexible polymethylene ( $n = 11$ ) spacer groups.

in dielectric constant of the medium cannot be ruled out, the results of steady-state and time-resolved fluorescence, CV, and NMR studies indicate the formation of a relatively planarized conformer of **1a** and **1c** upon  $\beta$ -CD encapsulation, as compared to dyads in the aqueous medium. In these systems, the spacer aryl group, with a dihedral angle of around 64.8° with respect to the acridine chromophore,<sup>17a</sup> undergoes a rotation and thereby becomes relatively planar, with a comparatively lower dihedral angle, when encapsulated inside the cavity. In support of this

view, we observed significantly decreased reduction potentials of the viologen moiety of dyads **2b** and **2c** with flexible spacer groups, indicating that these dyads do not undergo planarization but effective encapsulation as evidenced from photophysical, chiroptical, and electrochemical studies. The relative planarization of dyads **1a** and **1c** upon encapsulation in  $\beta$ -CD, as compared to the aqueous medium, was further unambiguously established through COSY and NOESY experiments. The viologen-linked conjugate **1a** showed no NOE peaks in D<sub>2</sub>O,



but in the presence of  $\beta$ -CD it exhibited strong positive NOE signals in the aromatic region, indicating the involvement of effective through-space interactions caused by planarization of the dyad.

## 5. Conclusions

In conclusion, we demonstrate the contrasting effects of flexible polymethylene and rigid aryl spacer groups on the photophysical and electrochemical properties of the novel viologen-linked acridine dyads **1a–c** and **2a–c**, when bound to  $\beta$ -CD. Upon  $\beta$ -CD complexation, the interaction between donor and acceptor moieties is inhibited in dyads **2a–c**, with flexible spacer groups, while it is significantly enhanced in the case of dyads **1a** and **1c**, with rigid aryl spacer groups. In the presence of  $\beta$ -CD, viologen-linked acridine dyads containing flexible spacer groups undergo unfolding of the sandwich-type folded structure, thereby resulting in a decreased rate of electron transfer, while the enhanced rates of electron transfer observed with systems having rigid aryl spacers is attributed to the unusual planarization of the dyad upon encapsulation in the  $\beta$ -CD cavity. This paper describes the first examples of  $\beta$ -CD-induced planarization of dyads, and the results presented are important in understanding interactions between donor–acceptor units and unusual effects of spacer groups and organized media, and also in the design of drug delivery systems and molecular machines.

**Acknowledgment.** We thank the Council of Scientific and Industrial Research and Department of Science and Technology (DST), Government of India, for financial support and Dr. N. V. Eldho and Dr. Joshy Joseph for their partial experimental assistance. This is Contribution PPG-181 from NIIST, Trivandrum.

**Supporting Information Available:** General experimental techniques and Figures S1–S10, showing experimental details of the changes in absorption, fluorescence, CD, CV, and fluorescence anisotropy of dyads **1a–c** and **2a–c** in the presence and absence of  $\beta$ -CD and micelles. This material is available free of charge via the Internet at <http://pubs.acs.org>.

## References and Notes

- (1) (a) Monti, S.; Sortino, S. *Chem. Soc. Rev.* **2002**, *31*, 287–300. (b) Douhal, A. *Science* **1997**, *276*, 221–222. (c) Ball, P. *Nature*, **2003**, *423*, 25–26. (d) Nepogodiev, S. A.; Stoddart, J. F. *Chem. Rev.* **1998**, *98*, 1959–1976. (e) Connors, K. A. *Chem. Rev.* **1997**, *97*, 1325–1357.
- (2) (a) Kalyanasundaram, K. In *Photochemistry in Microheterogeneous Systems*; Academic Press: Orlando, FL, 1987; pp 299–335. (b) Breslow, R.; Dong, S. D. *Chem. Rev.* **1998**, *98*, 1997–2011. (c) Li, S.; Purdy, W. C. *Chem. Rev.* **1992**, *92*, 1457–1490. (d) Komiyama, M. In *Cyclodextrins as Enzyme Models*; Atwood, J. L.; Davies, J. E.; MacNicol, D. D.; Vogtle, F., Eds.; Comprehensive Supramolecular Chemistry series; Pergamon: Oxford, U.K., 1996; Vol. 3, pp 401–421.
- (3) (a) Breslow, R. Hydrophobic and Antihydrophobic Effects on Organic Reactions in Aqueous Solution. In *Structure and Reactivity in Aqueous Solution*; Cramer, C. J.; Truhlar, D. G., Eds.; American Chemical Society: Washington, DC, 1994; pp 291–302. (b) Uekama, K.; Hirayama, F.; Irie, T. *Chem. Rev.* **1998**, *98*, 2045–2076.
- (4) (a) Rekharsky, M. V.; Inoue, Y. *Chem. Rev.* **1998**, *98*, 1875–1917. (b) D'Souza, V. T.; Lipkowitz, K. B. *Chem. Rev.* **1998**, *98*, 1741–1742.
- (5) Szejtli, J.; Osa, T. *Comprehensive Supramolecular Chemistry*; Elsevier: Oxford, U.K., 1996; Vol. 3.
- (6) (a) Takahashi, K. *Chem. Rev.* **1998**, *98*, 2013–2034. (b) Raymo, F. M.; Stoddart, J. F. *Chem. Rev.* **1999**, *99*, 1643–1663. (c) Wenz, G. *Angew. Chem., Int. Ed. Engl.* **1994**, *33*, 803–822. (d) Kawaguchi, Y.; Harada, A. *J. Am. Chem. Soc.* **2000**, *122*, 3797–3798.
- (7) Douhal, A. *Chem. Rev.* **2004**, *104*, 1955–1976.
- (8) Schneider, H. J.; Hacket, F.; Rudiger, V.; Ikeda, H. *Chem. Rev.* **1998**, *98*, 1755.
- (9) (a) Bakirci, H.; Zhang, X.; Nau, W. M. *J. Org. Chem.* **2005**, *70*, 39–46. (b) Szejtli, J. *Chem. Rev.* **1998**, *98*, 1743–1753. (c) Ikeda, H.; Nihei, T.; Ueno, A. *J. Org. Chem.* **2005**, *70*, 1237–1242.
- (10) (a) Park, J. W.; Song, H. E.; Lee, S. Y. *J. Phys. Chem. B* **2002**, *106*, 7186–7192. (b) Park, J. W.; Lee, B. A.; Lee, S. Y. *J. Phys. Chem. B* **1998**, *102*, 8209–8215. (c) Hwang, H. J.; Lee, S.; Park, J. W. *Bull. Korean Chem. Soc.* **2000**, *21*, 245–250. (d) Park, J. W.; Song, H. J. *Org. Lett.* **2004**, *6*, 24–26. (e) Park, J. W.; Lee, S. Y.; Song, H. J.; Park, K. K. *J. Org. Chem.* **2005**, *70*, 9505–9513.
- (11) (a) Yonemoto, E. H.; Kim, Y.; Schmehl, R. H.; Wallin, J. O.; Shoulders, B. A.; Richardson, B. R.; Haw, J. F.; Mallouk, T. E. *J. Am. Chem. Soc.* **1994**, *116*, 10557–10563. (b) Yonemura, H.; Kasahara, M.; Saito, H.; Nakamura, H.; Matsuo, T. *J. Phys. Chem.* **1992**, *96*, 5765–5770. (c) Yonemura, H.; Nojiri, T.; Matsuo, T. *Chem. Lett.* **1994**, 2097–2100. (d) Saito, H.; Yonemura, H.; Nakamura, H.; Matsuo, T. *Chem. Lett.* **1990**, 535–538. (e) Watanabe, M.; Nakamura, H.; Matsuo, T. *Bull. Chem. Soc. Jpn.* **1992**, *65*, 164–169.
- (12) Harada, A. *Acc. Chem. Res.* **2001**, *34*, 456–464.
- (13) Badjic, J. D.; Balzani, V.; Credi, A.; Silvi, S.; Stoddart, J. F. *Science* **2004**, *303*, 1845–1849.
- (14) Wasielewski, M. R. *Chem. Rev.* **1992**, *92*, 435–461.
- (15) Clark, C. D.; Debad, J. D.; Yonemoto, E. H.; Mallouk, T. E.; Bard, A. J. *J. Am. Chem. Soc.* **1997**, *119*, 10525–10531.
- (16) Yonemoto, E. H.; Saupe, G. B.; Schmehl, R. H.; Hubig, S. M.; Riley, R. L.; Iverson, B. L.; Mallouk, T. E. *J. Am. Chem. Soc.* **1994**, *116*, 4786–4795.
- (17) (a) Joseph, J.; Eldho, N. V.; Ramaiah, D. *J. Phys. Chem. B* **2003**, *107*, 4444–4450. (b) Joseph, J.; Eldho, N. V.; Ramaiah, D. *Chem.—Eur. J.* **2003**, *9*, 5926–5935. (c) Eldho, N. V.; Joseph, J.; Ramaiah, D. *Chem. Lett.* **2001**, 438–439.
- (18) Weber, G.; Teale, F. W. J. *Trans. Faraday Soc.* **1957**, *53*, 646–655.
- (19) Abiraj, K.; Srinivasa, G. R.; Gowda, C. *Synlett* **2004**, *5*, 877–879.
- (20) (a) Mazzaglia, A.; Angelini, N.; Lombardo, D.; Micali, N.; Patane, S.; Villari, V.; Scolaro, L. M. *J. Phys. Chem. B* **2005**, *109*, 7258–7265. (b) Sen, P.; Roy, D.; Mondal, S. K.; Sahu, K.; Ghosh, S.; Bhattacharyya, K. *J. Phys. Chem. B* **2005**, *109*, 9716–9722.
- (21) (a) Bakirci, H.; Zhang, X.; Nau, W. M. *J. Org. Chem.* **2005**, *70*, 39–46. (b) Joseph, J.; Kuruvilla, E.; Achuthan, A. T.; Ramaiah, D.; Schuster, G. B. *Bioconjugate Chem.* **2004**, *15*, 1230–1235. (c) Kuruvilla, E.; Ramaiah, D. *J. Phys. Chem. B* **2007**, *111*, 6549–6556. (d) Kubista, M.; Aakerman, B.; Nordén, B. *J. Phys. Chem.* **1988**, *92*, 2352–2356.
- (22) (a) Zhu, L.; Zhong, Z. L.; Anslyn, E. V. *J. Am. Chem. Soc.* **2005**, *127*, 4260–4269. (b) Wiskur, S. L.; Ait-Haddou, H.; Lavigne, J. J.; Anslyn, E. V. *Acc. Chem. Res.* **2001**, *34*, 963–972. (c) Jisha, V. S.; Arun, K. T.; Hariharan, M.; Ramaiah, D. *J. Am. Chem. Soc.* **2006**, *128*, 6024–6025. (d) Nau, W.; Zhang, X. *J. Am. Chem. Soc.* **1999**, *121*, 8022–8032.
- (23) Harries, D.; Rau, D. C.; Parsegian, V. A. *J. Am. Chem. Soc.* **2005**, *127*, 2184–2190.
- (24) (a) Bolas, P. L.; Kaifer, M. G.; Echegoyen, L. *Angew. Chem., Int. Ed.* **1998**, *37*, 216–247. (b) Hariharan, M.; Karunakaran, S. C.; Ramaiah, D. *Org. Lett.* **2007**, *9*, 417–420. (c) Neelakandan, P. P.; Hariharan, M.; Ramaiah, D. *Org. Lett.* **2005**, *7*, 5765–5768. (d) Neelakandan, P. P.; Hariharan, M.; Ramaiah, D. *J. Am. Chem. Soc.* **2006**, *128*, 11334–11335.
- (25) Mutz, M. W.; McLendon, G. L.; Wishart, J. F.; Gaillard, E. R.; Corin, A. F. *Proc. Natl. Acad. Sci. U.S.A.* **1996**, *93*, 9521–9526.
- (26) (a) Hariharan, M.; Joseph, J.; Ramaiah, D. *J. Phys. Chem. B* **2006**, *110*, 24678–24686. (b) Okhubo, K.; Yukimoto, K.; Fukuzumi, S. *Chem. Commun.* **2006**, 2504–2506. (c) Candias, L. P.; Steenken, S. *J. Am. Chem. Soc.* **1989**, *111*, 1094–1099. (d) Watanabe, T.; Honda, K. *J. Phys. Chem.* **1982**, *86*, 2617–2619.
- (27) (a) Goto, H.; Furusho, Y.; Yashima, E. *J. Am. Chem. Soc.* **2006**, *129*, 109–112. (b) Nelissen, H. F. M.; Kercher, M.; De Cola, L.; Feiters, M. C.; Nolte, R. J. M. *Chem.—Eur. J.* **2002**, *8*, 5407–5414.
- (28) Wasielewski, M. R.; Gaines, G. L.; O'Neil, M. P.; Svec, W. A.; Niemczyk, M. P.; Prodi, L.; and Gosztola, D. In *Dynamics and Mechanisms of Photoinduced Electron Transfer and Related Phenomena*; Mataga, N.; Okada, T.; Masuhara, H., Eds.; Elsevier: Amsterdam, 1992; pp 87–103.
- (29) Sessler, J. L.; Wang, B.; Harriman, A. *J. Am. Chem. Soc.* **1995**, *117*, 704–714.
- (30) Verhoeven, J. W. *Pure Appl. Chem.* **1990**, *62*, 1585–1596.
- (31) Le, T. P.; Rogers, J. E.; Kelly, L. A. *J. Phys. Chem. A* **2000**, *104*, 6778–6785.
- (32) (a) Schuette, J. M.; Ndou, T.; de la Pena, A. M.; Greene, K. L.; Williamson, C. K.; Warner, I. M. *J. Phys. Chem.* **1991**, *95*, 4897–4902. (b) Schuette, J. M.; Ndou, T.; de la Pena, A. M.; Mukundan, S., Jr.; Warner, I. M. *J. Am. Chem. Soc.* **1993**, *115*, 292–298.
- (33) Mirzozian, A.; Kaifer, A. E. *Chem.—Eur. J.* **1997**, *3*, 1052–1058.